Available online at www.sciencedirect.com
ScienceDirect
Neuromuscular Disorders 21 (2011) 345–352
www.elsevier.com/locate/nmd

# Myonuclear breakdown in sporadic inclusion body myositis is accompanied by DNA double strand breaks

Makoto Nishii [a], Satoshi Nakano [a,b,*], Seika Nakamura [a], Reika Wate [a], Akiyo Shinde [a], Satoshi Kaneko [a], Hirofumi Kusaka [a]

[a] *Department of Neurology and Brain Medical Research Center, Kansai Medical University, Japan*
[b] *Department of Neurology, Osaka City General Hospital, Japan*

Received 29 September 2010; received in revised form 18 January 2011; accepted 2 February 2011

**Abstract**

Rimmed vacuoles in sporadic inclusion body myositis (s-IBM) contain nuclear remnants. We sought to determine if the nuclear degeneration seen in s-IBM is associated with DNA damage. In muscle biopsy specimens from ten patients with s-IBM and 50 controls, we immunolocalized 1) phosphorylated histone H2AX (γ-H2AX), which is a sensitive immunocytochemical marker of DNA double-strand breaks and 2) DNA-PK, which is an enzyme involved in double-strand break repair. In s-IBM, vacuolar peripheries often showed strong immunoreactivity to γ-H2AX and the three components of DNA-PK (DNA-PKcs, Ku70, and Ku80). A triple fluorescence study of Ku70, emerin, and DNA displayed nuclear breakdown and it suggested impaired nuclear incorporation of Ku70. The percentage of positive nuclei for γ-H2AX was significantly higher in vacuolated fibers than non-vacuolated fibers in s-IBM, or fibers in polymyosits. We hypothesize that a dysfunction of nuclear envelope may cause nuclear fragility, double-strand breaks and impaired nuclear transport in s-IBM.


*Keywords:* Inclusion body myositis; Rimmed vacuole; DNA double strand breaks (DSB); Nuclear breakdown

## 1. Introduction

Sporadic inclusion body myositis (s-IBM) is the primary cause of acquired myopathy in patients over 50-years old, but no effective therapy has yet been found [1,2]. The histopathological hallmarks of s-IBM consist of mononuclear cell infiltration, muscle fibers with congophilic inclusions, and rimmed vacuoles. Several studies showed nuclear components in the rimmed vacuoles (e.g., a single-stranded DNA binding protein of nuclear origin [3], emerin [4,5], lamin A/C [4] and histone H1 with DNA [5]). The findings indicate that the vacuoles may result from nuclear breakdown.

Terminally differentiated cells do not possess a replication-associated DNA repair mechanism, making them particularly sensitive to DNA damage [6]. Mature muscle cells are such terminally differentiated cells. In a muscle cell culture study, the exposure of differentiated myocytes to hydrogen peroxide resulted in the accumulation of foci of phosphorylated histone H2AX (γ-H2AX) [7], which is a sensitive marker of a serious form of DNA damage, DNA double strand breaks (DSB) [8]. DSB are produced by reactive oxygen species (ROS), ionizing radiation, and other genotoxic agents. Histone H2AX, a variant of histone H2A, is rapidly phosphorylated at Ser 139 in the chromatin region surrounding a DSB [9]. Immunocytochemical staining of γ-H2AX has been broadly applied to reveal DNA damage caused by cancer and other cellular stresses [8,10]. DNA-PK is an enzyme involved in the initial step of

* Corresponding author. Address: Department of Neurology, Osaka City General Hospital, 2-13-22 Miyakojima hondori, Miyakojima-ku, Osaka 534-0021, Japan. Tel.: +81 66929 1221, fax: +81 66929 1091.
*E-mail addresses:* s-nakano@hospital.city.osaka.jp, nakanos@takii.kmu.ac.jp (S. Nakano).

0960-8966/$ - see front matter © 2011 Elsevier B.V. All rights reserved.
doi:10.1016/j.nmd.2011.02.004

the DSB repair process, non-homologous end joining (NHEJ), which does not require DNA replication, and therefore NHEJ is the predominant DNA repair mechanism in terminally differentiated cells [11,12]. DNA-PK consists of a catalytic subunit (DNA-PKcs) and two regulatory subunits (Ku70 and Ku80). The binding of heteroduplexes of Ku70 and Ku80 to DSB sites initiates the repair process [13,14]. In the current paper, we examine whether DSB are associated with myonuclear breakdown in s-IBM.

Note that DSB is different from the apoptotic DNA fragmentation that has been scarcely detected in the s-IBM muscles [15]. In DSB, DNA breaks occur directly and randomly by radiation or other genotoxic agents, whereas apoptotic DNA fragmentation takes place at a late stage of programmed cell death, in which endonucleases sever DNA strands at regular lengths. Apoptotic DNA fragmentation is not subject of repair or is not usually labeled with anti-γ-H2AX antibody.

## 2. Materials and methods

### 2.1. Patients

We studied muscle biopsy specimens from 10 patients (58–82 years old, 8 men and 2 women) who fulfilled the clinical, electromyographic, and histopathological criteria for s-IBM [16]. The muscle sections displayed cell infiltration surrounding non-necrotic fibers, congophilic inclusions and rimmed vacuoles in each patient. All s-IBM patients showed slowly progressive muscular symptoms (disease duration: 3.8 ± 2.9 years; mean ± standard deviation [SD], range: 0.5–9 years). None of these patients had received immunotherapy before the muscle biopsy. Specimens from five patients without pathologic alterations served as non-pathologic controls. For controls of other neuromuscular diseases, we used 45 muscle biopsies from patients with polymyositis ($n = 10$), dermatomyositis (8), dystrophinopathy (3), dysferlinopathy (3), mitochondrial encephalomyopathy (5), myotonic dystrophy type I (1), neurogenic muscular atrophy (5), oculopharyngeal muscular dystrophy (5), myopathy with autophagic vacuoles of an undetermined etiology (1), rhabdomyolysis (1), hypokalemic vacuolar myopathy (2), and colchicine myopathy (1). The above diagnoses were based on a clinical examination, family history, electromyography, and muscle biopsy studies. Polymyositis and dermatomyositis were diagnosed using conventional criteria [17]. The polymyositis sections contained several to many non-necrotic fibers surrounded by mononuclear cells, and the dermatomyositis sections demonstrated perifascicular atrophy or perimysial infiltration of inflammatory cells. This study was performed with the compliance of the internal review board of our institution.

### 2.2. Immunohistochemistry

Table 1 shows the primary antibodies applied and their concentrations. Immunohistochemical studies were performed as previously described [18]. Briefly, sections were fixed in cold acetone and then in 4% paraformaldehyde in 0.1 M phosphate buffer (pH 7.4) before being blocked and incubated overnight at 4 °C with the primary antibody. The sections were then incubated with a biotin-labeled secondary antibody and developed using the avidin–biotin complex (ABC) immunoperoxidase method (Vector Laboratories, Burlingame, CA) with 3,3′-diaminobenzidine as the coloring agent. Next, the slides were lightly counterstained with hematoxylin for the quantitation of positive nuclei. The control experiments involved the omission of the primary antibody or the substitution of the primary antibody for non-immune mouse or rabbit IgG. We immunostained 12 or more sections from different individuals at a time, and the duration of color development was fixed. The specificity of antibodies for γ-H2AX and Ku70 was also tested in immunoblotting.

For triple-color immunofluorescence studies, the sections were incubated with anti-Ku70 plus anti-emerin antibodies followed by incubation with appropriate secondary antibodies for triple fluorescence (Chemicon International, Temecula, CA). The slides were mounted with Vectashield (Vector) containing 1.5 μg/mL of the nuclear DNA marker 4′,6-diamidino-2-phenylindole (DAPI) and examined with confocal imaging using the LSM510-META system (Carl Zeiss, Jena, Germany). As controls, we performed a single-color fluorescence study using each antibody or DAPI alone and confirmed the specificity of the secondary antibodies and filters.

Table 1
List of primary antibodies.

| Antigen | Type | Clone/ID | Source | Concentration |
|---|---|---|---|---|
| γ-H2AX | MMA | JBW301 | Upstate | 1 μg/mL |
| Ku70 | MMA | 4C2–1A6 | Abnova | 1 μg/mL |
| Ku80 | MMA | 111 | Abcam | 1:500 |
| DNA-PKcs | RPA | PC127 | Calbiochem | 5 μg/mL |
| Emerin | RPA | FL-254 | Santa-Cruz Biotec | 1 μg/mL |
| HNE | MMA | HNEJ-2 | JaICA | 20 μg/mL |
| iNOS | RPA | sc-651 | Santa-Cruz Biotec | 4 μg/mL |
| LAMP-2 | MMA | H4B4 | Santa-Cruz Biotec | 4 μg/mL |

MMA: mouse monoclonal antibody; RPA: rabbit polyclonal antibody.

### 2.3. Immunoelectron microscopy

Preembedding immunoelectron microscopy was performed using the immunogold method with silver-enhancement [19]. Cryostat sections, prepared from s-IBM biopsy specimens that had been stored at −80 °C, were attached to a slide glass, fixed in 4% paraformaldehyde, and incubated with the anti-Ku70 antibody at a 100-fold dilution. The sections were then incubated with a secondary antibody (goat IgG, Fab' fragment) coupled with 1.4 nm gold particles (Nanoprobes Inc., Yaphank, NY). The sample-bound gold particles were then silver-enhanced using the HQ-silver kit (Nanoprobes) at room temperature for 12–14 min according to the manufacturer's instructions. Then, the samples were postfixed with 0.5% osmium oxide in 0.1 M phosphate-buffer at pH 7.4, before being dehydrated in a graded series of ethanol (50%, 70%, 90%, and 100%) and propylene oxide, and embedded in epoxy resin. Ultrathin sections were then cut, stained with uranyl acetate and lead citrate, and examined with a JEM-1400A electron microscope (JEOL Ltd., Tokyo, Japan).

### 2.4. Quantitation

For quantitation of the γ-H2AX-positive myonuclei in the non-pathologic controls, a mean of 342 randomly selected photographed nuclei were inspected for each sample. In s-IBM, a mean of 42.3 vacuolated fibers were photographed per patient. For each vacuolated fiber, we surveyed γ-H2AX-positivity in vacuoles and nuclei. To quantitate the positive nuclei in non-vacuolated fibers, we analyzed a mean of 266 nuclei in 97 randomly selected muscle fibers in each s-IBM patient. In polymyositis, we analyzed a total of 1657 randomly selected myonuclei. In

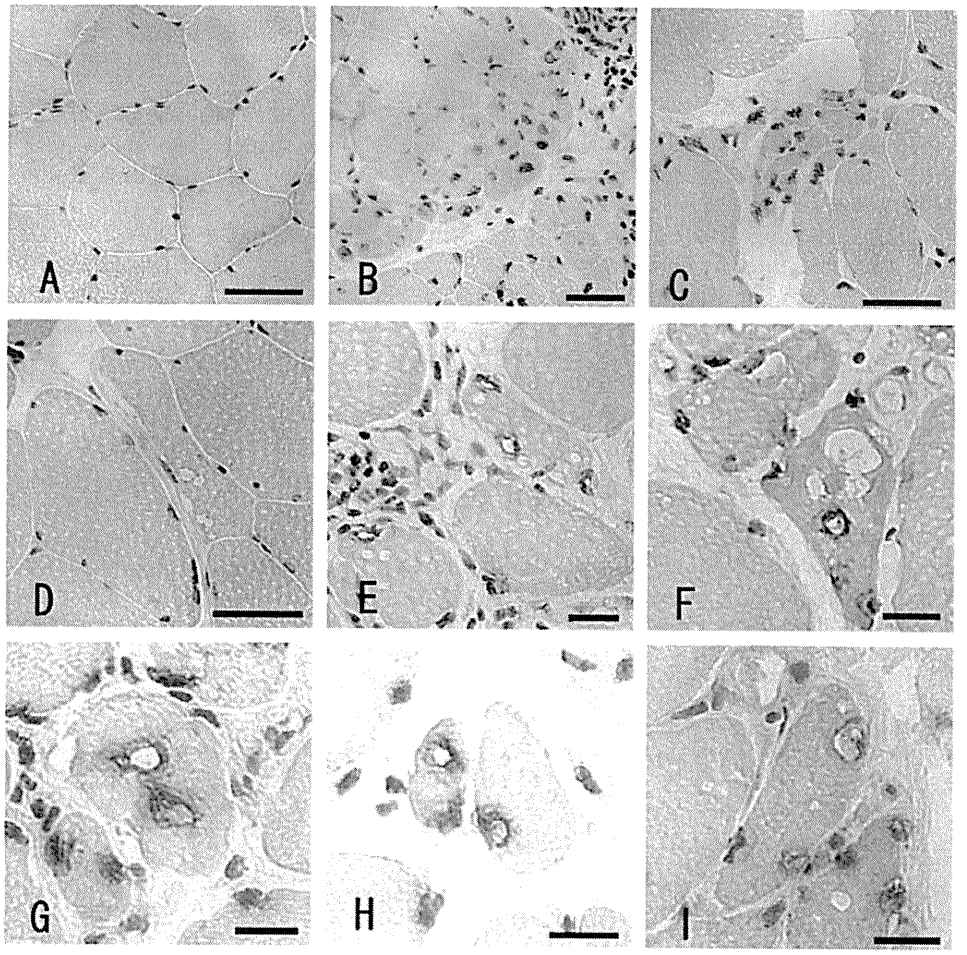


Fig. 1. A–F: Localization of γ-H2AX, which is induced upon the occurrence of DNA double-strand breaks (DSB); in controls (A–D); and sporadic inclusion body myositis (s-IBM) (E–F). Immuno-peroxidase method, lightly counterstained with hematoxylin to localize nuclei. (A) non-pathologic control, (B) perifascicular atrophy in dermatomyositis, (C) grouped atrophy in neurogenic muscular atrophy, and (D) oculopharyngeal muscular dystrophy (OPMD). The myonuclei in A show no or trace immunoreaction to γ-H2AX. The nuclei of the atrophic fibers in B and C are strongly positive for γ-H2AX. In D, the vacuoles in OPMD are negative for γ-H2AX. In E & F, the vacuolar rims and myonuclei in s-IBM contain strongly positive γ-H2AX products. Some mononuclear cells in the inflammatory exudates in E are positive. G–I: Localization of the three components of DNA-PK (G: Ku70, H: Ku80 and I: DNA-PKcs) in vacuolated fibers in s-IBM. Vacuolar peripheries and nuclei display positive immunoreactivity for each component of DNA-PK. Bar = 50 μm (A–D); 20 μm (E–I).

s-IBM DNA-PKcs, we examined a total of 393 vacuolated fibers with 950 nuclei and 1953 myonuclei in non-vacuolated fibers. As it was sometimes difficult to differentiate between the nuclei of invading/surrounding mononuclear cells and myonuclei, we excluded muscle fibers surrounding inflammatory cells from the nucleus calculation. We categorized nuclei as positive when a brown color was clearly discernible against lightly-stained hematoxylin.

## 3. Results

### 3.1. Increased expression of the DNA double strand break (DSB) marker γ-H2AX in s-IBM vacuolated fibers

In the non-pathologic controls, a small number of myonuclei showed a weakly positive reaction to γ-H2AX ($n = 5$; $6.0 \pm 1.8\%$, mean ± standard deviation [SD]. Range: 3.97–8.05) (Fig. 1A). In polymyositis and dermatomyositis, the nuclei in regenerating fibers were positive for γ-H2AX. The nuclei in perifascicular atrophic fibers in cases of dermatomyositis were strongly positive (Fig. 1B), and positive myonuclei were also found in other fibers in polymyositis and dermatomyositis. A proportion of the cells in inflammatory exudates were positive for γ-H2AX. In neurogenic muscular atrophy, strongly reactive nuclei were usually found in atrophic angulated fibers (Fig. 1C), and the nuclei at pyknotic nuclear clumps showed increased reactivity for γ-H2AX. In other neuromuscular diseases, the nuclei at nuclear clumps such as those observed in myotonic dystrophy showed increased reactivity for γ-H2AX, and the nuclei in ragged-red fibers in mitochondrial encephalomyopathy and those of regenerating fibers in various myopathies were strongly positive for γ-H2AX. Vacuoles in hypokalemic myopathy, myopathy with autophagic vacuoles, colchicine myopathy, and OPMD were negative for γ-H2AX (Fig. 1D).

In s-IBM, a proportion of fibers contained vacuoles that were partially or entirely lined by positive immunoreactivity (Fig. 1E and F). Table 2 shows the percentage of (1) vacuolated fibers vs. total fibers and (2) fibers containing γ-H2AX positive vacuoles vs. total vacuolated fibers in patients with s-IBM ($n = 10$; $74.0 \pm 13.0\%$, mean ± SD). The nuclei in vacuolated fibers displayed strong γ-H2AX-positive reactivity, and the percentage of positive nuclei was significantly higher in vacuolated fibers than in non-vacuolated fibers (Table 1) ($p < 0.01$; paired Student's t-test). In polymyositis, the percentage of γ-H2AX-positive nuclei ($n = 10$; $23.3 \pm 7.4\%$, mean ± SD) was similar to that in the non-vacuolated fibers in s-IBM, but lower than that in the vacuolated fibers ($p < 0.01$; Student's t-test).

The results of immunoblotting using this anti-γ-H2AX antibody showed several positive bands including ubiquitinated forms of γ-H2AX (Fig. 2) [20].

### 3.2. Detection of the DSB repair enzyme DNA-PK in s-IBM

In s-IBM, all of the DNA-PK components (DNA-PKcs, Ku70, and Ku80) were found in vacuolar peripheries as well as being strongly expressed in nuclei, consistent with the results for γ-H2AX (Fig. 1G, H and I). As for DNA-PKcs, $70.6 \pm 14.0\%$ (mean ± SD) of vacuolated fibers contained positive vacuoles for DNA-PKcs. The percentage of positive nuclei for DNA-PKcs was significantly higher in vacuolated fibers than in non-vacuolated fibers ($61.7 \pm 10.6\%$, mean ± SD, vs. $32.5 \pm 10.2\%$: $p < 0.01$; paired t-test). Ku70 was often found to form several round or comma-shaped cytoplasmic inclusions in vacuolated fibers and other fibers. We confirmed the relative localization of Ku70, the nuclear envelope, and DNA in a triple-fluorescence study in five patients with s-IBM, five patients with polymyositis, and patients with other diseases. In polymyositis and other controls, Ku70 was confined to within the emerin boundary, even when the Ku70-signal was very intense (Fig. 3A). In vacuolated fibers in s-IBM, although Ku70 was often localized to the nuclei, it was also found in vacuolar peripheries, around the nuclei, and in the cytoplasm (Fig. 3B and C). In a few instances, cytoplasmic Ku70-positive granules were associated with nuclear frag-

Table 2
Quantitation.

| s-IBM Pt number | Vacuolated fibers/total fibers (%) | γ-H2AX positive fibers/vacuolated fibers (%) | Positive nuclei in | |
|---|---|---|---|---|
| | | | Vacuolated fibers (%) | Non-vacuolated fibers (%) |
| 1 | 18.6 | 87.2 | 64.0 | 24.5 |
| 2 | 21.0 | 82.9 | 64.0 | 29.0 |
| 3 | 5.0 | 69.6 | 64.5 | 39.4 |
| 4 | 4.2 | 76.5 | 70.3 | 23.8 |
| 5 | 7.2 | 89.5 | 81.4 | 38.2 |
| 6 | 23.0 | 76.8 | 65.0 | 22.1 |
| 7 | 6.6 | 47.1 | 58.8 | 8.5 |
| 8 | 7.6 | 74.6 | 56.5 | 25.2 |
| 9 | 4.2 | 58.1 | 58.2 | 24.9 |
| 10 | 7.6 | 78.3 | 63.9 | 21.6 |
| Mean ± SD | 10.5 ± 7.3 | 74.0 ± 13.0 | 64.7 ± 7.1* | 25.7 ± 8.8 |

* The percentages for vacuolated fibers are significantly higher than those for non-vacuolated fibers ($p < 0.01$).

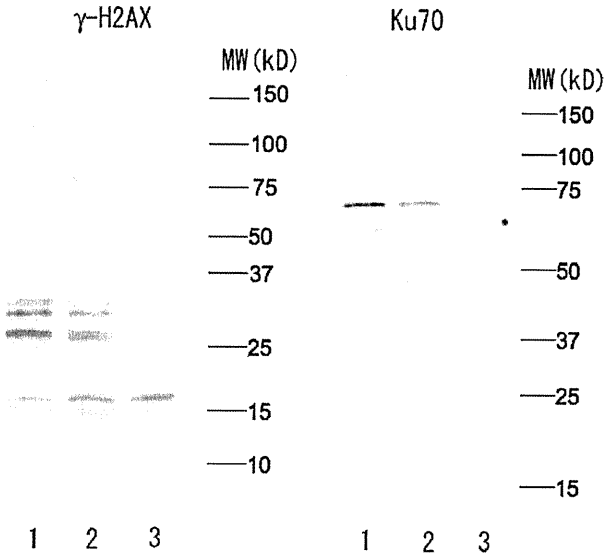


Fig. 2. Tests for the antibody specificity in immunoblotting. Muscle homogenates in control patients were segregated through polyacrylamide gel electrophoresis and immunoblotted using anti-γ-H2AX (left) and Ku70 (right) antibodies. The molecular weights of γ-H2AX and Ku70 are 15 kDa and 70 kDa, respectively. In γ-H2AX, patient 1 and 2, the extra bands between 25 kDa and 37 kDa correspond to the ubiquitinated forms [20]. In Ku70, patient 1 and 2, positive bands appear around its molecular weight.

ments, indicating nuclear breakdown. Ku70-positive deposits were sometimes found around intact nuclei (Fig. 3D).

Immunoblotting of muscle homogenates with the anti-Ku70 antibody showed a clear band around the molecular weight (Fig. 2).

### 3.3. Localization of HNE, iNOS, and LAMP-2

ROS is an inducer of DSB in muscle cells and oxidative stress may be associated with vacuolar formation [21], so we tested 4-hydroxy-2-noenal (HNE), a product of lipid peroxidation by ROS [22], and iNOS, a marker of oxidative stress that was previously found to be increased in vacuolated fibers [21]. HNE and iNOS were increased not only in some vacuolated fibers in s-IBM, but also in perifascicular atrophic fibers in dermatomyositis and ragged red fibers. In non-vacuolated fibers in s-IBM, atrophic fibers in neurogenic muscular atrophy, and pyknotic nuclear clumps, the two ROS markers were not increased.

Several studies indicated that rimmed vacuoles are lysosomes in origin [23,24]. In this study, we observed that vacuoles in s-IBM usually showed positive for the lysosome marker LAMP-2, as described previously [23]. A dual fluorescence study using antibodies against LAMP-2 and emerin showed frequent association of these two markers in the vacuoles in s-IBM.

### 3.4. Immuno-electron microscopy of Ku70

In the ultrastructural study of Ku70 in s-IBM, we detected Ku70-positive granules in some nuclei. Ku70-positive granules were often found in the vacuolar spaces of

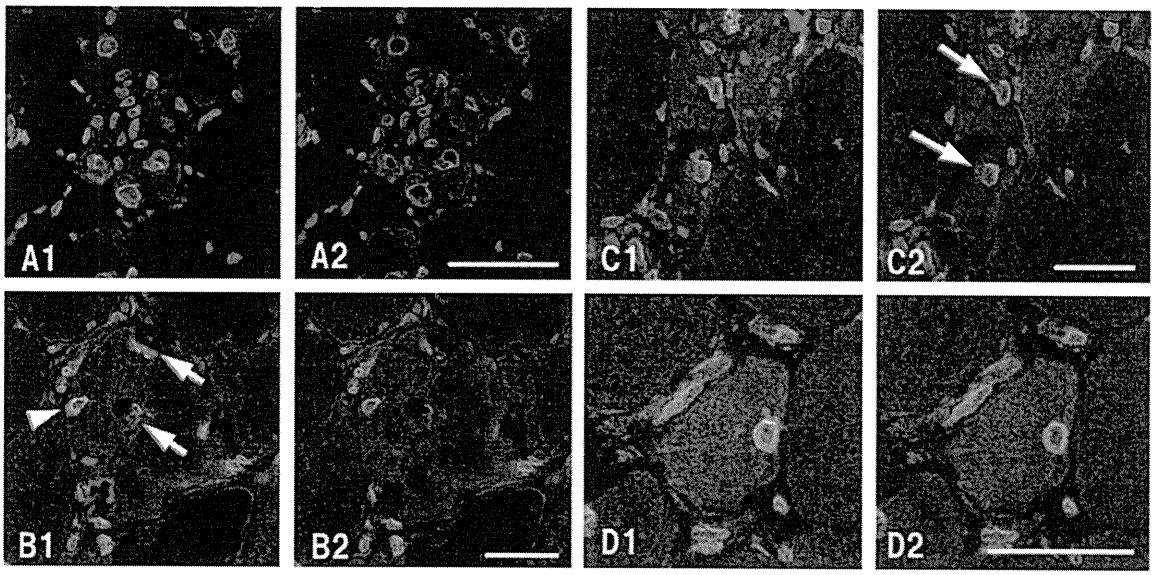


Fig. 3. Triple fluorescence study. Ku70 (red), emerin (green), and DNA (DAPI: blue). A: Regenerating fibers. B to D: s-IBM. A1–D1: overlay of the three colors. A2–D2: emerin plus DNA. (A) Ku70-positive deposits are largely confined to the area surrounded by emerin. (B) A vacuolated fiber contains a nucleus abutted by deposits of Ku70 (arrow head). Fragments of Ku70-positive deposits intermingle with remnants of emerin or DNA (arrows). The figures indicate nuclear breakdown and impaired incorporation of Ku70 into the nucleus. (C) Muscle fibers with numerous cytoplasmic deposits of Ku70 and breaks in the nuclear envelope (arrows). (D) Ku70-positive deposits surrounding a nucleus with an intact circle of emerin. This figure shows that nuclear import of Ku70 is impaired even in the early phase of nuclear breakdown in s-IBM. Bar = 25 μm.

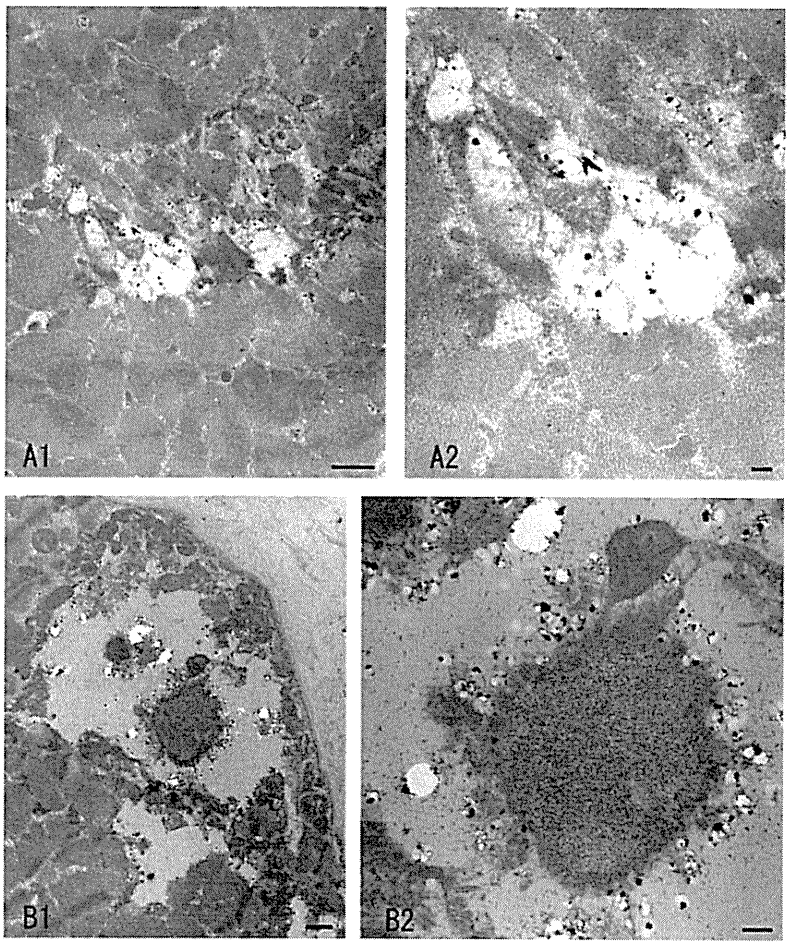


Fig. 4. Immunoelectron microscopy of Ku70, a regulatory component of DNA-PK. (A1) Deposits of Ku70 in cytoplasmic spaces. (A2) Higher magnification of A1. The positive reactivity may correspond to the cytoplasmic inclusion of Ku70 in immunofluorescence. (B1) Ku70 surrounding electron-dense round bodies. (B2) Higher magnification of one body shows granular structures inside with a peripheral dense zone. According to the triple fluorescence results, such as those shown in Fig. 3, the round body corresponds to a degenerating nucleus, and the electron micrograph may illustrate that the nucleus cannot incorporate Ku70. Bar = 1 μm (A1 & B1), 200 nm (A2), 500 nm (B2).

various sizes, sometimes combined with degenerative products (Fig. 4A). Ku70-positive products were also found to be attached to something like degenerating nuclear structures that contained no Ku70 (Fig. 4B), which may have corresponded to nuclei surrounded by Ku70-positive deposits in the immunofluorescence study (Fig. 3B, arrowhead).

## 4. Discussion

### *4.1. Findings in s-IBM*

In the current study, we showed that the percentage of DSB-positive nuclei was significantly higher in vacuolated fibers than in other fibers in s-IBM. This finding suggests that nuclear breakdown along with the accumulation of DSB occurs in muscle cells in s-IBM. Moreover, we detected figures suggesting impaired nuclear import of Ku70. Nuclear translocation of Ku proteins is important for DBS repair, and a deficiency in nuclear translocation caused hypersensitivity against X-ray irradiation due to the lack of DBS repair in a cell culture study [25]. Therefore, we hypothesize that defects in Ku70 nuclear import accelerate DSB formation.

As DSB occur in other disease conditions without nuclear breakdown, additional factors may be involved in the nuclear changes seen in s-IBM. There is evidence that nuclear envelope dysfunction can cause both mechanical fragility of the nucleus and DNA damage. Lamins are proteins of nuclear intermediate filaments that comprise the lamina, the meshwork supporting inner nuclear membranes. Mutations in the genes that encode lamins and emerin (a lamin-associated protein) cause Emery–Dreifuss muscular dystrophy and a number of different diseases collectively called laminopathies [26]. In several laminopathies, blebbing of the nuclei in cultured fibroblasts can be seen, and it is hypothesized that such mutations result in fragile and mechanically unstable nuclei [27]. Emerin mutations can cause myopathy with rimmed vacuoles [28,29]. Besides structural integrity, the lamina is also involved in

various other processes, such as replication and gene transcription, which are intimately associated with DNA damage repair. Accordingly, impaired DNA repair has been found in several laminopathies. Fibroblasts possessing a laminopathy mutation show an excessive amount of unrepaired DNA damage, as evidenced by γ-H2AX immunohistochemistry [30]. Furthermore, lamins are important in the spatial rearrangement of nuclear pore complexes and therefore nuclear protein transport. Nuclear protein import is reduced in cells expressing lamin A mutants [31]. In the current study, we detected figures suggestive of impaired nuclear import of Ku70. Defects of nuclear import have been suggested for the mechanism of cytoplasmic accumulation of enzymes (e.g., ERK [32] and MKP-1 [33]) and nuclear molecules (e.g., pElk-1 [5,32] and TDP-43 [34]) in s-IBM. In summary, dysfunctional lamins can explain the nuclear breakdown, accumulation of DSB, and impaired nuclear transport observed in s-IBM. A specific stressor predicted in this disease [35] may affect lamins or other nuclear envelope components. Alternatively, the nuclear envelope might become fragile by aging. Cell nuclei from old individuals exhibit defects similar to those of cells from Hutchinson–Gilford progeria syndrome, which is caused by mutations of lamin A [36]. Likewise, nuclear pore complexes are not turned over in differentiated cells, and age-related alterations in nuclear pore complexes affect nuclear integrity [37]. Moreover, several studies have indicated an age-dependent decline in DNA repair capacity [38]. We suspect that these age-associated changes in nuclear envelope integrity and DNA repair mechanisms may predispose the muscles of the elderly to s-IBM pathology. In this context, the initial inducer of DSB in s-IBM muscle may be the same as that in polymyositis.

We found products that were positive for the lysosome marker LAMP-2 in rimmed vacuoles, indicating that they also originate from lysosomes. Moreover, we found that the LAMP-2-positive products were frequently associated with emerin. These findings suggest the induction of autophagy to process broken-down nuclei. In the muscle of laminopathy patients and emerin-null mice, it has been shown that autophagosomes/autolysosomes are involved in the degradation of damaged nuclear components [39].

### *4.2. Findings in other diseases*

Recent studies indicate an up-regulation of type 1 interferon inducible proteins in dermatomyositis muscle with perifascicular atrophy [40]. A prolonged stimulation of type 1 interferon (β-interferon) induces ROS and DNA damage response in culture study [41]. Therefore, the strong myonuclear γ-H2AX staining and excessive levels of ROS found in perifascicular atrophy might correspond with this hypothesis. The strong myonuclear γ-H2AX staining found in ragged red fibers may have been induced by increased ROS caused by mitochondrial dysfunction. Although the small angulated fibers show positive γ-H2AX reactivity, the majority of these fibers were negative for HNE and iNOS. Our results suggest that γ-H2AX histochemistry is more sensitive to detect ROS injury than the two markers or that other genotoxic stresses attack on muscle cells during degeneration. Contrary to the case in s-IBM, vacuoles in OPMD, which may originate from the nucleus and show some histone H1-positivity [5], were negative for γ-H2AX. This result suggests that simple nuclear breakdown does not induce DSB. We found a strong γ-H2AX reaction in a proportion of cells in inflammatory exudates. As DSB occurs during V(D)J recombination in lymphocyte development [11], γ-H2AX-positive cells may be active in gene recombination.

## Acknowledgments

This work was supported by Grant-in-Aids from the Japan Society for the Promotion of Science and from the Ministry of Health, Labour, and Welfare for Research on intractable diseases.

## References

[1] Dalakas MC. Sporadic inclusion body myositis–diagnosis, pathogenesis and therapeutic strategies. Nat Clin Pract Neurol 2006;2:437–47.
[2] Needham M, Mastaglia FL. Sporadic inclusion body myositis: a continuing puzzle. Neuromuscul Disord 2008;18:6–16.
[3] Nalbantoglu J, Karpati G, Carpenter S. Conspicuous accumulation of a single-stranded DNA binding protein in skeletal muscle fibers in inclusion body myositis. Am J Pathol 1994;144:874–82.
[4] Greenberg SA, Pinkus JL, Amato AA. Nuclear membrane proteins are present within rimmed vacuoles in inclusion-body myositis. Muscle Nerve 2006;34:406–16.
[5] Nakano S, Shinde A, Fujita K, Ito H, Kusaka H. Histone H1 is released from myonuclei and present in rimmed vacuoles with DNA in inclusion body myositis. Neuromuscul Disord 2008;18:27–33.
[6] Lee Y, McKinnon PJ. Responding to DNA double strand breaks in the nervous system. Neuroscience 2007;145:1365–74.
[7] Narciso L, Fortini P, Pajalunga D, et al. Terminally differentiated muscle cells are defective in base excision DNA repair and hypersensitive to oxygen injury. Proc Natl Acad Sci U S A 2007;104:17010–5.
[8] Nakamura A, Sedelnikova OA, Redon C, et al. Techniques for gamma-H2AX detection. Methods Enzymol 2006;409:236–50.
[9] Kinner A, Wu W, Staudt C, Iliakis G. Gamma-H2AX in recognition and signaling of DNA double-strand breaks in the context of chromatin. Nucleic Acids Res 2008;36:5678–94.
[10] Dickey JS, Redon CE, Nakamura AJ, Baird BJ, Sedelnikova OA, Bonner WM. H2AX: functional roles and potential applications. Chromosoma 2009;118:683–92.
[11] O'Driscoll M, Jeggo PA. The role of double-strand break repair–insights from human genetics. Nat Rev Genet 2006;7:45–54.
[12] Mahaney BL, Meek K, Lees-Miller SP. Repair of ionizing radiation-induced DNA double-strand breaks by non-homologous end-joining. Biochem J 2009;417:639–50.
[13] Mari PO, Florea BI, Persengiev SP, et al. Dynamic assembly of end-joining complexes requires interaction between Ku70/80 and XRCC4. Proc Natl Acad Sci U S A 2006;103:18597–602.
[14] Weterings E, Chen DJ. DNA-dependent protein kinase in nonhomologous end joining: a lock with multiple keys? J Cell Biol 2007;179:183–6.
[15] Hutchinson DO. Inclusion body myositis: abnormal protein accumulation does not trigger apoptosis. Neurology 1998;51:1742–5.
[16] Griggs RC, Askanas V, DiMauro S, et al. Inclusion body myositis and myopathies. Ann Neurol 1995;38:705–13.

[17] Dalakas MC, Hohlfeld R. Polymyositis and dermatomyositis. Lancet 2003;362:971–82.
[18] Nakano S, Shinde A, Ito H, Ito H, Kusaka H. Messenger RNA degradation may be inhibited in sporadic inclusion body myositis. Neurology 2005;65:420–5.
[19] Mizoguchi A, Yano Y, Hamaguchi H, et al. Localization of Rabphilin-3A on the synaptic vesicle. Biochem Biophys Res Commun 1994;202:1235–43.
[20] Pinato S, Scandiuzzi C, Arnaudo N, Citterio E, Gaudino G, Penengo L. RNF168, a new RING finger, MIU-containing protein that modifies chromatin by ubiquitination of histones H2A and H2AX. BMC Mol Biol 2009;10:55.
[21] Yang CC, Alvarez RB, Engel WK, Askanas V. Increase of nitric oxide synthases and nitrotyrosine in inclusion-body myositis. Neuroreport 1996;8:153–8.
[22] Uchida K. A lipid-derived endogenous inducer of COX-2: a bridge between inflammation and oxidative stress. Mol Cells 2008;25:347–51.
[23] Tsuruta Y, Furuta A, Furuta K, Yamada T, Kira J, Iwaki T. Expression of the lysosome-associated membrane proteins in myopathies with rimmed vacuoles. Acta Neuropathol 2001;101:579–84.
[24] Kumamoto T, Ueyama H, Tsumura H, Toyoshima I, Tsuda T. Expression of lysosome-related proteins and genes in the skeletal muscles of inclusion body myositis. Acta Neuropathol 2004;107:59–65.
[25] Okui T, Endoh D, Kon Y, Hayashi M. Deficiency in nuclear accumulation of G22p1 and Xrcc5 proteins in hyper-radiosensitive Long–Evans Cinnamon (LEC) rat cells after X irradiation. Radiat Res 2002;157:553–61.
[26] Capell BC, Collins FS. Human laminopathies: nuclei gone genetically awry. Nat Rev Genet 2006;7:940–52.
[27] Goldman RD, Shumaker DK, Erdos MR, et al. Accumulation of mutant lamin A causes progressive changes in nuclear architecture in Hutchinson–Gilford progeria syndrome. Proc Natl Acad Sci U S A 2004;101:8963–8.
[28] Paradas C, Márquez C, Gallardo E, et al. X-linked Emery–Dreifuss muscular dystrophy and vacuoles: an immunohistochemical characterization. Muscle Nerve 2005;32:61–5.
[29] Fidziańska A, Rowińska-Marcińska K, Hausmanowa-Petrusewicz I. Coexistence of X-linked recessive Emery–Dreifuss muscular dystrophy with inclusion body myositis-like morphology. Acta Neuropathol 2004;107:197–203.
[30] Liu B, Wang J, Chan KM, et al. Genomic instability in laminopathy-based premature aging. Nat Med 2005;11:780–5.
[31] Busch A, Kiel T, Heupel WM, Wehnert M, Hübner S. Nuclear protein import is reduced in cells expressing nuclear envelopathy-causing lamin A mutants. Exp Cell Res 2009;315:2373–85.
[32] Nakano S, Shinde A, Kawashima S, Nakamura S, Akiguchi I, Kimura J. Inclusion body myositis: expression of extracellular signal-regulated kinase and its substrate. Neurology 2001;56:87–93.
[33] Nakano S, Shinde A, Ito H, Ito H, Kusaka H. MAP kinase phosphatase-1 is induced in abnormal fibers in inclusion body myositis. Neurology 2003;61:322–6.
[34] Salajegheh M, Pinkus JL, Taylor JP, et al. Sarcoplasmic redistribution of nuclear TDP-43 in inclusion body myositis. Muscle Nerve 2009;40:19–31.
[35] Banwell BL, Engel AG. AlphaB-crystallin immunolocalization yields new insights into inclusion body myositis. Neurology 2000;54:1033–41.
[36] Scaffidi P, Misteli T. Lamin A-dependent nuclear defects in human aging. Science 2006;312:1059–63.
[37] D'Angelo MA, Raices M, Panowski SH, Hetzer MW. Age-dependent deterioration of nuclear pore complexes causes a loss of nuclear integrity in postmitotic cells. Cell 2009;136:284–95.
[38] Gorbunova V, Seluanov A, Mao Z, Hine C. Changes in DNA repair during aging. Nucleic Acids Res 2007;35:7466–74.
[39] Park YE, Hayashi YK, Bonne G, et al. Autophagic degradation of nuclear components in mammalian cells. Autophagy 2009;5:795–804.
[40] Salajegheh M, Kong SW, Pinkus JL, et al. Interferon-stimulated gene 15 (ISG15) conjugates proteins in dermatomyositis muscle with perifascicular atrophy. Ann Neurol 2010;67:53–63.
[41] Moiseeva O, Mallette FA, Mukhopadhyay UK, Moores A, Ferbeyre G. DNA damage signaling and p53-dependent senescence after prolonged beta-interferon stimulation. Mol Biol Cell 2006;17:1583–92.

Neurol Sci
DOI 10.1007/s10072-011-0814-y

ORIGINAL ARTICLE

# A dysphagia study in patients with sporadic inclusion body myositis (s-IBM)

**Ken-ya Murata · Ken Kouda · Fumihiro Tajima · Tomoyoshi Kondo**

Received: 18 May 2011 / Accepted: 24 September 2011


**Abstract** The nature of the swallowing impairment in patients with sporadic inclusion body myositis (s-IBM) has not been well characterized. In this study, we examined ten consecutive s-IBM patients using videofluoroscopy (VF) and computed pharyngoesophageal manometry (CPM). The patients were divided into two groups: patients with complaint and without complaint of dysphagia. VF results indicated pharyngeal muscle propulsion (PP) at the hypopharyngeal and upper esophagus sphincter (UES) in all s-IBM patients. Patients without complaint of dysphagia showed a mild degree of PP, whereas a severe form of PP was observed in patients with complaint of dysphagia. CPM revealed that negative pressure during UES opening was not observed in the s-IBM patients with complaint of dysphagia. Incomplete opening and PP at the UES were observed in all s-IBM patients. These results indicate that the dysphagic processes occur subclinically in s-IBM patients who may not report swallowing impairments.

**Keywords** Inclusion body myositis · Videofluoroscopy · Pharyngoesophageal manometry · Pharyngeal muscle propulsion · Upper esophagus sphincter

K. Murata (✉) · T. Kondo
Department of Neurology, Wakayama Medical University,
840-1 Kimii-dera, Wakayama 641-8510, Japan
e-mail: kemurata@wakayama-med.ac.jp

K. Kouda · F. Tajima
Department of Rehabilitation Medicine,
Wakayama Medical University, 840-1 Kimii-dera,
Wakayama 641-8510, Japan

Published online: 13 October 2011

## Introduction

Sporadic inclusion body myositis (s-IBM) is an inflammatory myopathy characterized by selectivity of muscle involvement, finger flexor and/or quadriceps femoris involvement, moderate elevation of muscle enzyme concentrations, and a progressive corticosteroid-resistant course. Muscle histopathology shows rimmed-vacuoles, groups of atrophic angular fibers, and endomysial mononuclear cell infiltrations.

Dysphagia has been reported in s-IBM patients. As described by Lotz et al. [1], 10% of the s-IBM patients complained of dysphagia at onset, and 40% of the patients suffered from dysphagia at the time of diagnosis. Patients with progressive dysphagia have a significantly worse functional class rating and poorer quality of life than patients with non-progressive dysphagia [2]. However, the nature of the swallowing impairment in s-IBM and other inflammatory myopathies has not been well characterized. Previous studies suggest that improper contraction of the pharyngeal muscles or cricopharyngeal muscle dysfunction may result in functional obstruction due to dysphagia [3–6].

The purpose of this study was to assess the frequency and nature of dysphagia in s-IBM patients and to identify a possible therapy for dysphagia associated with s-IBM.

## Methods

Study subjects were ten consecutive patients (mean age 70.5 ± 7.1 years; 5 males and 5 females) who fulfilled the proposed diagnostic criteria for s-IBM [7] at the Department of Neurology in Wakayama Medical University between January 2000 and July 2011. Muscle biopsy studies were performed on the quadriceps femoris or biceps

brachii in all patients. All specimens were frozen rapidly in isopentane that was chilled in dry ice, and the specimens were stored at −80°C before examination. 5-micron serial sections of each specimen were stained with hematoxylin and eosin (H&E) and modified Gomori Trichrome stain. Muscle biopsy results showed mononuclear cell infiltration around non-necrotic fibers and rimmed-vacuoles in all patients. Swallowing problems were assessed by a personal structured interview, videofluoroscopy (VF) and computed pharyngoesophageal manometry (CPM). All subjects provided written informed consent to the procedures in this study and the ethics committee at the Wakayama Medical University approved all methods used in the study.

### Videofluoroscopy (VF)

All ten patients underwent oropharyngeal videofluoroscopic swallowing examination. Patients were placed upright, and the oropharynx was viewed in lateral and anterior-posterior projections. 3 ml of liquid barium and paste barium were administered by teaspoon. Swallowing examinations were repeated in different upright positions. Dysphagia severity was scored using the 8-point Penetration Aspiration Scale (PAS) [8].

### Computed pharyngoesophageal manometry (CPM)

CPM was performed in all ten patients. For CPM, a sequential computer manometry system (PC polygraph) (Medtronic, Medtronic Parkway, Minneapolis) with a 4-intraluminal pressure transducer assembly (Mui Scientific, Mississauga, Ontario) was used with the recording sites set at 5 cm apart. The assembly was placed transnasally, and recording sites were chosen at the following four points: oropharynx, hypopharynx, upper esophageal sphincter (UES), and proximal esophagus (Fig. 3a). We evaluated UES pressure and pharyngeal and esophageal peristalsis during barium swallowing.

## Results

### Clinical findings

Ten patients were examined in this study. The subjects were divided into two groups: patients with complaint of dysphagia (Group A) and patients without complaint of dysphagia (Group B) (Table 1). Group A consisted of three men and two women who complained of dysphagia in the form of regurgitation of liquids and problems with solids. Group B consisted of two men and three women who did not complain of dysphagia. Mean age at examination was 73.8 ± 6.8 years in Group A and 67.2 ± 5.7 years in Group B. The average duration of the disease was 11.0 ± 5.4 years in Group A and 11.0 ± 1.3 years in Group B. There were no statistical differences in mean age, duration of disease and creatine kinase levels between the two groups. Other than one woman (Patient 3) in Group A, all of the patients used a cane or caster walker when walking.

### Videofluoroscopy (VF)

Videofluoroscopy results indicated that all patients had a normal oral phase of swallowing and abnormalities in the pharyngeal phase. While barium material did not enter the airway in all patients in Group B, the barium material entered the airway, remained above the vocal folds, and

**Table 1** s-IBM patient profiles

| Patient | Sex | Complaint of dysphagia | PAS | Age | Duration of disease (years) | Aid for walking | CK (IU/L) | Complications |
|---|---|---|---|---|---|---|---|---|
| Group A | | | | 73.8 ± 6.8 | 11.0 ± 5.4 | | 432 | |
| 1 | M | (+) | 2 | 74 | 14 | Cane | 691 | HT |
| 2 | F | (+) | 2 | 79 | 12 | Walker | 482 | HT, LS |
| 3 | F | (+) | 2 | 64 | 6 | None | 353 | Sjogren Synd |
| 4 | M | (+) | 2 | 83 | 4 | Walker | 186 | Hepatitis C |
| 5 | M | (+) | 2 | 69 | 19 | Cane | 447 | HT |
| Group B | | | | 67.2 ± 5.7 | 11.0 ± 1.3 | | 492 | |
| 6 | M | (−) | 1 | 77 | 12 | Cane | 482 | HT, DM |
| 7 | F | (−) | 1 | 62 | 9 | Cane | 503 | HT |
| 8 | M | (−) | 1 | 62 | 12 | Cane | 482 | None |
| 9 | F | (−) | 1 | 70 | 12 | Cane | 643 | None |
| 10 | F | (−) | 1 | 65 | 10 | Cane | 350 | None |

*HT* Hypertension, *LS* Lumbar spondylosis, *DM* Diabetes mellitus

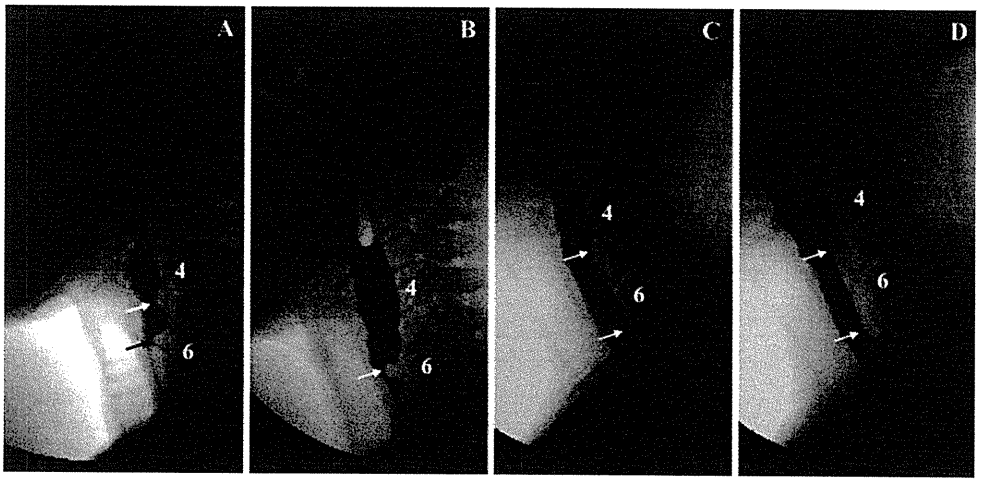


**Fig. 1** Videofluoroscopic study in s-IBM patients using paste barium (**a**, **c**) and liquid barium (**b**, **d**). Pharyngeal muscle propulsions (PP) (*arrows*) were observed in Patient 2 (**a**, **b**) and Patient 4 (**c**, **d**). The degree of PP and the narrowing at the upper esophageal sphincter region in Patient 2 is more severe than that in Patient 4. The sites and shapes varied between using paste or liquid barium (**a**, **b** and **c**, **d**)

was ejected from the airway in all patients in Group A. The 8-point PAS showed a score of 2 in all patients in Group A and 1 in all patients in Group B (Table 1). Pharyngeal phase abnormalities included decreased epiglottic deflection and residue in the epiglottic vallecula and piriform recesses. Pharyngeal muscle propulsion (PP) was indicated at the UES in all ten patients without reference to dysphagia (Figs. 1, 2; Table 2). Although, the PP sites in VF ranged from C3 to C7 vertebral levels, PP shapes and sites varied between using liquid and paste barium (Figs. 1a–d, 2a, b). Patients in Group B showed a mild degree of PP, whereas a severe form of PP was observed in all five patients in Group A. An insufficiency of the UES opening was also observed in Group A patients. In addition, prominence of a segment of the hypopharyngeal sphincter muscles was observed in Patient 1 in Group A (Fig. 2a; Table 2).

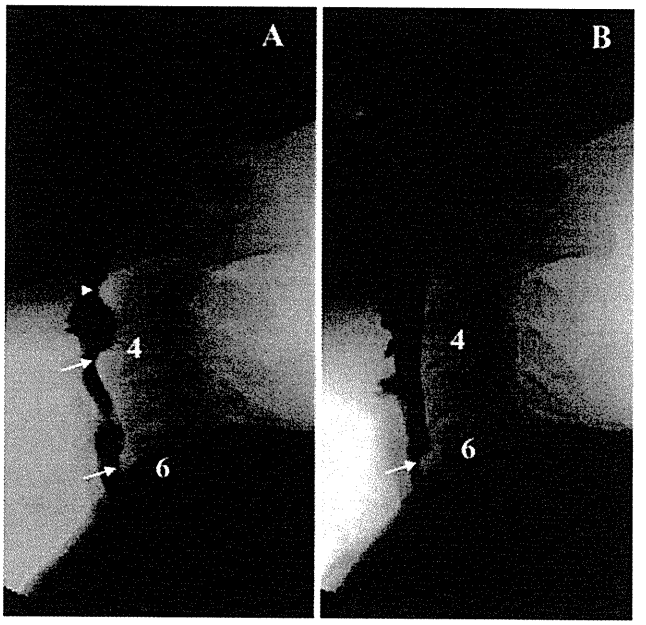


**Fig. 2** Videofluoroscopic study in s-IBM patients using paste barium (**a**) and liquid barium (**b**). Pharyngeal muscle propulsions (PP) (*arrows*) and a cephalad prominence (CP) (*arrow head*) were observed in Patient 1 (**a**, **b**). The sites and shapes of PP and CP varied between using paste or liquid barium (**a**, **b**)

## Computed pharyngoesophageal manometry (CPM)

In the normal control subjects, the pharyngeal peak pressure at the oropharynx and hypopharynx elevated simultaneously (Fig. 3b-1, 2). The pharyngeal pressure at the oropharynx was higher than that at the hypopharynx. Contrary to the high pharyngeal pressure in the oropharynx and hypopharynx, the pressure at the UES decreased until the UES opened (nadir deglutitive UES pressure) (Fig. 3b-3, arrow). After the barium paste passed through the entrance of the UES, pharyngeal pressure at the UES increased and pushed the paste to the upper esophagus (Fig. 3b-3).

In the s-IBM patients, the pressure at the oropharynx and hypopharynx was very low compared with that of the normal controls (Fig. 3c-1, 2). In addition, the negative pressure during UES opening (nadir deglutitive UES pressure) observed in the normal controls was not observed in the s-IBM patients with dysphagia (Fig. 3c-3). Manometric recordings in all s-IBM patients revealed a lack of oropharyngeal peristaltic activity, a decreased hypopharyngeal peristalsis, and a reduced peak of post-deglutitive UES pressure, while the esophageal resting pressure was normal. In addition, all s-IBM patients in Group A demonstrated no deglutitive UES relaxation in the CPM study.

**Table 2** Videofluoroscopic and manometric findings in ten patients with s-IBM

| Pt | Group | Videofluoroscopy | | | |
|---|---|---|---|---|---|
| | | PP site | Insufficiency of UES opening | Pooling site of barrium | Manometry |
| 1 | A | C3, C4-5, C6-7 | (+) | EV, piriform | No UES relaxation |
| 2 | | C4-5, C5-6, C6 | (+) | EV, piriform | Decreased oro-hypopharyngeal pressure |
| 3 | | C5-6, C6-7 | (+) | EV | Decreased deglutitive UES pressure |
| 4 | | C5-6 | (+) | EV, piriform | |
| 5 | | C6-7 | (++) | EV, piriform | |
| 6 | B | C3-4 | (−) | EV | Incomplete UES relaxation |
| 7 | | C5-7 | (−) | None | Decreased oro-hypopharyngeal pressure |
| 8 | | C5-6 | (−) | EV, piriform | Decreased deglutitive UES pressure |
| 9 | | C4-5, C6-7 | (−) | None | Incomplete UES relaxation |
| 10 | | C5-6 | (−) | EV | Incomplete UES relaxation |

*PP* pharyngeal muscle propulsion, *UES* upper esophageal sphincter, *EV* epiglottic vallecula, *piriform* piriform recess

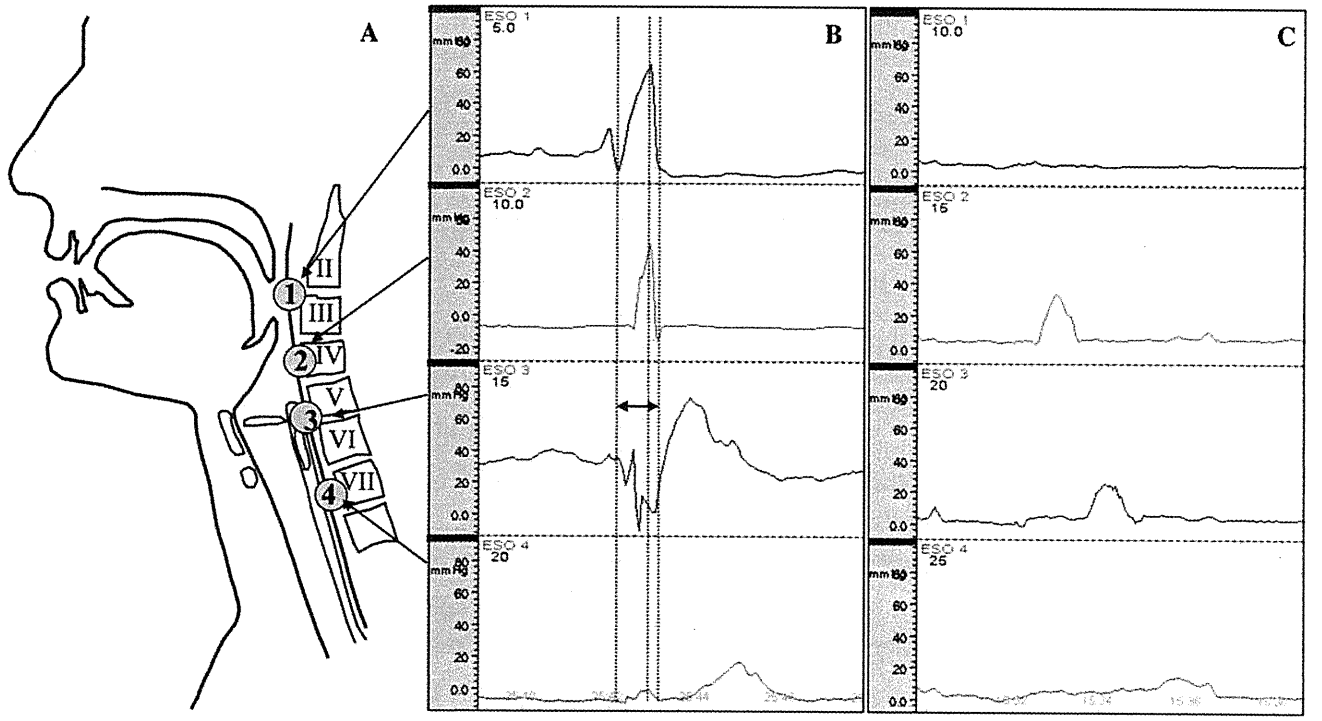


**Fig. 3** Manometry **a** Manometry study using simultaneous 4-channel pressure recording during 3 ml barium swallowing. **b** Manometric findings in a healthy control subject: *channel 1* oropharynx, *channel 2* hypopharynx, *channel 3* UES, *channel 4* proximal esophagus. **c** Patient 3: Pharyngoesophageal manometry during swallowing solid barium paste. The pressure at the oropharyngx, hypopharyngx and UES is none or very low compared with that of normal controls. UES negative pressure during UES opening (nadir deglutitive UES pressure), which was observed in normal controls (**b**, *arrow*), was not observed

In contrast, incomplete UES relaxation was observed in Group B patients (Table 2).

## Discussion

The consequences of dysphagia include weight loss, the need for modified food consistency and non-oral feeding. Pulmonary infections occur in patients with dysphagia, and aspiration pneumonia is considered a main cause of death in s-IBM patients. We observed PP at the UES and/or hypopharyngeal muscle in all ten s-IBM patients. PP was first reported as a prominent cricopharyngeal impression at the cricopharyngeal muscles [9], and these findings were observed not only in s-IBM patients, but also in mitochondria myopathy patients [10]. PP is also defined as

cricopharyngeal achalasia. We observed PP at the hypopharyngeal muscles in Patient 1, and this PP has been named cephalad prominence [11]. Because PP in VF is observed in front of the vertebral discs, it may be considered the result of disc prolapse. In this study, the PP shapes and sites varied between using liquid and paste barium. Therefore, we conclude that the PP observed here did not represent the result of disc prolapse.

PP was observed at the UES in all ten s-IBM patients, while only five patients (Group A) complained of dysphagia. The local esophageal diameter reduction by PP in Group A was >50% at the UES during swallowing. The degree of PP in Group A was more severe than that of Group B (Fig. 1a–d). In addition, the five patients in Group A showed insufficiency of the UES opening in VF. PP is revealed as barium manages to go through the non-extended pharynx. It represents improper dilation of the pharyngeal muscles during barium passing. A dilation problem of the pharyngeal muscles can occur with the patient being unaware of swallowing difficulties. Although, there was a positive relationship between the severity of PP and the insufficiency of UES opening, PP does not induce cricopharyngeal obstruction. PP represents only the result of dilation problems of pharyngeal musculature.

The lack of negative UES pressure (nadir deglutitive UES pressure) in the s-IBM patients with dysphagia may explain swallowing difficulties. Incomplete pharyngeal musculature opening at the UES during swallowing may have a number of different causes, including impaired relaxation or spasm of the UES, hyperplasia and hypertrophy or fibrosis of the cricopharyngeal muscles, weakness of the suprahyoid muscles, and failure of neural inhibition of tonic sphincter contraction [12]. An examination of cricopharyngeal muscle biopsies of one patient was reported at the time of cricopharyngeal myotomy [4, 13]. Numerous small, round atrophic muscle fibers were observed which varied in size. Because the cricopharyngeal muscles have a sphincteric function, atrophic cricopharyngeal muscles failed to push foods toward the upper esophagus. In our manometry study, post-deglutitive UES pressure was observed, but the peak pressure was greatly reduced. Low pressure at the oropharynx and hypopharynx, and hypo-oropharyngeal peristaltic activities induced problems with the propulsion of the bolus through the sphincter muscles. In addition, there was a marked increase in endomysial connective tissue, some replacement by fat, and proliferative connective tissue. In s-IBM patients in Group A, nadir deglutitive UES pressure was not observed. This finding suggests that endomysial proliferative connective tissue prevented the extension and relaxation of the UES.

The prevalence of s-IBM in Asian populations including Japan has not been examined. Recently, a national survey study revealed that the number of s-IBM patients in Japan is estimated to be around 1,250 and that the prevalence of s-IBM is 9.83 per million [14]. We examined ten patients, representing 0.8% of all s-IBM patients in Japan. Although the number of patients was very low and results of our study are limited in significance, our study revealed a tendency in s-IBM patients with dysphagia.

Recently, cricopharyngeal myotomy was selected to reduce dysphagia in s-IBM patients [15]. The aim of the myotomy is to remove the impaired UES relaxation, which is not overcome by decreased PP. Indeed, myotomy has shown to be useful in improving dysphagia associated with UES hyperactivities in s-IBM, however, other therapies, such as intravenous immunoglobulin [16] or botulinum toxin A [17], and balloon dilation have been employed for s-IBM patients with dysphagia.

The combination test using VF and manometry is needed to assess the preservation of sphincter muscle strength and the efficacy of each therapy. Deglutitive pharyngoesophageal functions should be examined routinely in all s-IBM patients even if they do not complain of dysphagia.

## References


1. Lotz BP, Engel AG, Nishino H, Stevens JC, Litchy WJ (1989) Inclusion body myositis. Observations in 40 patients. Brain 112(Pt 3):727–747
2. Houser SM, Calabrese LH, Strome M (1998) Dysphagia in patients with inclusion body myositis. Laryngoscope 108:1001–1005
3. Wintzen AR, Bots GT, de Bakker HM, Hulshof JH, Padberg GW (1988) Dysphagia in inclusion body myositis. J Neurol Neurosurg Psychiatry 51:1542–1545
4. Danon MJ, Friedman M (1989) Inclusion body myositis associated with progressive dysphagia: treatment with cricopharyngeal myotomy. Can J Neurol Sci 16:436–438
5. Dietz F, Logeman JA, Sahgal V, Schmid FR (1980) Cricopharyngeal muscle dysfunction in the differential diagnosis of dysphagia in polymyositis. Arthritis Rheum 23:491–495
6. Kagen LJ, Hochman RB, Strong EW (1985) Cricopharyngeal obstruction in inflammatory myopathy (polymyositis/dermatomyositis). Report of three cases and review of the literature. Arthritis Rheum 28:630–636
7. Griggs RC, Askanas V, DiMauro S, Engel A, Karpati G, Mendell JR, Rowland LP (1995) Inclusion body myositis and myopathies. Ann Neurol 38:705–713
8. Rosenbek JC, Robbins JA, Roecker EB, Coyle JL, Wood JL (1996) A penetration-aspiration scale. Dysphagia 11:93–98
9. Seaman WB (1966) Cineroentgenographic observations of the cricopharyngeus. Am J Roentgenol Radium Ther Nucl Med 96:922–931
10. Kornblum C, Broicher R, Walther E, Seibel P, Reichmann H, Klockgether T, Herberhold C, Schroder R (2001) Cricopharyngeal achalasia is a common cause of dysphagia in patients with mtDNA deletions. Neurology 56:1409–1412
11. Shapiro J, Martin S, DeGirolami U, Goyal R (1996) Inflammatory myopathy causing pharyngeal dysphagia: a new entity. Ann Otol Rhinol Laryngol 105:331–335

12. Cook IJ, Blumbergs P, Cash K, Jamieson GG, Shearman DJ (1992) Structural abnormalities of the cricopharyngeus muscle in patients with pharyngeal (Zenker's) diverticulum. J Gastroenterol Hepatol 7:556–562
13. Verma A, Bradley WG, Adesina AM, Sofferman R, Pendlebury WW (1991) Inclusion body myositis with cricopharyngeus muscle involvement and severe dysphagia. Muscle Nerve 14:470–473
14. Suzuki N, Aoki M, Mori-Yoshimura M, Hayashi YK, Nonaka I, Nishino I (2011) Increase in number of sporadic inclusion body myositis (sIBM) in Japan. J Neurol. doi:10.1007/s00415-011-6185-8
15. St Guily JL, Moine A, Perie S, Bokowy C, Angelard B, Chaussade S (1995) Role of pharyngeal propulsion as an indicator for upper esophageal sphincter myotomy. Laryngoscope 105:723–727
16. Cherin P, Pelletier S, Teixeira A, Laforet P, Simon A, Herson S, Eymard B (2002) Intravenous immunoglobulin for dysphagia of inclusion body myositis. Neurology 58:326
17. Liu LW, Tarnopolsky M, Armstrong D (2004) Injection of botulinum toxin A to the upper esophageal sphincter for oropharyngeal dysphagia in two patients with inclusion body myositis. Can J Gastroenterol 18:397–399

# 平成23年度　班会議プログラム

厚生労働科学研究費補助金　難治性疾患克服研究事業

# 封入体筋炎（IBM）の臨床病理学的調査および診断基準の精度向上に関する研究班
# (H22-難治-一般-117)

## 平成23年度　研究班会議プログラム

研究代表者：　東北大学大学院医学系研究科　神経内科

青木　正志

日　　時　　平成24年1月 28日(土) 14:00～16:45

会　　場　　東北大学病院　仮管理棟4階　第一会議室

〒980-8574 宮城県仙台市青葉区星陵町1-2

TEL：022-717-7810(会議室)/ 7189 (医局)

お願い：演題発表時間15分（発表10分、討論5分）
発表者はご自身のPCをご持参くださいますようお願いいたします。

研究班事務局：加藤 昌昭、鈴木 直輝、伊藤 詩織
〒980-8574 宮城県仙台市青葉区星陵町1-1　東北大学神経内科
TEL 022-717-7189　FAX 022-717-7192

**開会挨拶および本研究班について　　14:00～14:10　　研究代表者　　青木 正志**

**封入体筋炎に関する班員研究発表　　14:10～16:30**

**Session I　　14:10～14:55　　座　長　　西野 一三**

**1. 封入対筋炎に対する IVIg の効果および評価法の検討（14:10～14:25）**

研 究 分 担 者：森 まどか
所　　属：国立精神・神経医療研究センター病院　神経内科
研 究 協 力 者：○西川 敦子(にしかわ あつこ)[1)]、森 まどか[1)]、 山本 敏之[1)]、大矢 寧[1)]、
西野 一三[2)]、村田 美穂[1)]
研究協力者所属：1）国立精神・神経医療研究センター病院　神経内科
2）国立精神・神経医療研究センター神経研究所　疾病研究第一部

**2. 封入体筋炎患者の画像診断（14:25～14:40）**

研 究 分 担 者：○村田 顕也（むらた けんや）
所　　属：和歌山県立医科大学　神経内科
研 究 協 力 者：三輪 英人[1)]、近藤 智善[1)]
研究協力者所属：1）和歌山県立医科大学　神経内科

**3. 封入体筋炎における筋細胞核障害の研究（14:40～14:55）**

研 究 分 担 者：日下 博文
所　　属：関西医科大学　神経内科
研 究 協 力 者：○中野 智（なかの さとし）[1,2)]、中村 聖香[1,2)]
研究協力者所属：1）大阪市立総合医療センター　神経内科
2）関西医科大学　神経内科

Session Ⅱ　　14:55～15:40　　座　長　　村田 顕也

**4. 封入体筋炎と肥大型心筋症を合併し、Myosin binding protein C3 遺伝子異常を認めた一剖検例 (14:55～15:10)**

研 究 分 担 者：樋口 逸郎
所　　属：鹿児島大学大学院　医歯学総合研究科　神経内科　老年病学
研 究 協 力 者：○稲森 由恵（いなもり ゆきえ）[1]、橋口 昭大[1]、白石 匡史[1]、東 桂子[1]、井上 輝彦[2]、三山 吉夫[2]、高嶋 博[1]
研究協力者所属：1）鹿児島大学大学院　医歯学総合研究科　神経内科　老年病学
2）大悟病院　老年期精神疾患センター

**5. 封入体筋炎骨格筋組織における家族性 ALS 関連分子の関与 (15:10～15:25)**

研 究 分 担 者：○山下 賢（やました さとし）
所　　属：熊本大学医学部附属病院　神経内科
研 究 協 力 者：木村 円[1]、俵 望[1]、坂口 秀哉[1]、中間 達也[1]、松尾 圭将[1]、前田 寧[1]、平野 照之[1]、内野 誠[1]
研究協力者所属：1）熊本大学医学部附属病院　神経内科

**6. 封入体筋炎との鑑別を要した非典型例の検討 (15:25～15:40)**

研 究 分 担 者：梶 龍兒
所　　属：徳島大学　神経内科
研 究 協 力 者：○松井 尚子（まつい なおこ）[1]、高松 直子[1]、寺澤 由佳[1]、和泉 唯信[1]
研究協力者所属：1）徳島大学　神経内科

＊＊＊＊＊＊＊＊　　コーヒーブレイク　　15:40～16:00　　＊＊＊＊＊＊＊＊

Session Ⅲ　　16:00～16:40　　座　　長　　青木 正志

**7. 東アジアにおける IBMPFD (16:00～16:15)**

研 究 分 担 者：○西野 一三（にしの いちぞう）
所　　属：国立精神・神経医療研究センター神経研究所　疾病研究第一部
研 究 協 力 者：石 志鴻[1]、三橋 里美[1]、後藤 加奈子[1]、野口 悟[1]、林 由起子[1]
研究協力者所属：1）国立精神・神経医療研究センター神経研究所　疾病研究第一部

**8. 封入体筋炎研究班、3年間のまとめ（16:15〜16:40）**

研究代表者：○青木 正志（あおき まさし）
所　　属：東北大学大学院医学系研究科　神経内科
研究協力者：加藤 昌昭[1)]、竪山 真規[1)]、割田 仁[1)]、井泉 瑠美子[1)]、鈴木 直輝[1)]、
島倉 奈緒子[1)]、安藤 里紗[1)]、新井 法子[1)]、吉田 美智子[1)]、高橋 俊明[2)]、
西野 一三[3)]、森 まどか[4)]、日下 博文[5)]、樋口 逸郎[6)]、近藤 智善[7)]、
山下 賢[8)]、内野 誠[8)]、梶 龍兒[9)]
研究協力者所属：1）東北大学神経内科
2）国立西多賀病院
3）国立精神・神経医療研究センター神経研究所　疾病研究第一部
4）国立精神・神経医療研究センター病院　神経内科
5）関西医科大学　神経内科
6）鹿児島大学医学部・歯学部附属病院　神経内科
7）和歌山県立医科大学　神経内科
8）熊本大学　神経内科
9）徳島大学　神経内科

**閉会挨拶**　　**16:40〜16:45**　　**研究代表者　青木 正志**

**移動**

**研究打合せ会議**　　**18：00〜 勝山館　楓（かえで）**